



Poly (N-isopropylacrylamide) microgel-based etalons and etalon arrays for determining the molecular weight of polymers in solution

Molla R. Islam and Michael J. Serpe

Citation: *APL Mater.* **1**, 052108 (2013); doi: 10.1063/1.4829975

View online: <http://dx.doi.org/10.1063/1.4829975>

View Table of Contents: <http://scitation.aip.org/content/aip/journal/aplmater/1/5?ver=pdfcov>

Published by the [AIP Publishing](#)

Articles you may be interested in

[Poly\(vinylidene fluoride-hexafluoropropylene\) polymer electrolyte for paper-based and flexible battery applications](#)

AIP Advances **6**, 065206 (2016); 10.1063/1.4953811

[Revisit to phase diagram of poly\(N-isopropylacrylamide\) microgel suspensions by mechanical spectroscopy](#)

J. Chem. Phys. **140**, 024908 (2014); 10.1063/1.4861426

[Structural properties of thermoresponsive poly\(N-isopropylacrylamide\)-poly\(ethyleneglycol\) microgels](#)

J. Chem. Phys. **136**, 214903 (2012); 10.1063/1.4723686

[High-density electrostatic carrier doping in organic single-crystal transistors with polymer gel electrolyte](#)

Appl. Phys. Lett. **88**, 112102 (2006); 10.1063/1.2186513

[Ionic conduction in 70 - MeV C⁵⁺ -ion-irradiated poly\(vinylidene fluoride-co-hexafluoropropylene\)-based gel polymer electrolytes](#)

J. Appl. Phys. **98**, 043514 (2005); 10.1063/1.2030417

NEW Special Topic Sections

NOW ONLINE
Lithium Niobate Properties and Applications:
Reviews of Emerging Trends

AIP Applied Physics Reviews

The advertisement features a blue background with a molecular structure of spheres and rods. On the left, there is a thumbnail image of the journal cover for Applied Physics Reviews, showing a diagram of a layered structure and a graph. The text is prominently displayed in white and yellow.

Poly (*N*-isopropylacrylamide) microgel-based etalons and etalon arrays for determining the molecular weight of polymers in solution

Molla R. Islam and Michael J. Serpe^a

Department of Chemistry, University of Alberta, Edmonton, T6G 2G2 Alberta, Canada

(Received 3 July 2013; accepted 23 October 2013; published online 15 November 2013)

Positively and/or negatively charged poly (*N*-isopropylacrylamide)-based microgels were deposited on a single substrate and isolated regions of Au overlayers were deposited on top of the microgels. Each spatially isolated Au overlayer region had a different thickness to make an etalon array. We found that areas with a thin Au overlayer (5 nm) responded to a range of polymer molecular weights (MW), while areas with a thick overlayer (35 nm) can only respond to low molecular weight polyelectrolytes. By comparing the optical responses of the device's individual array elements, a good approximation of the polyelectrolyte MW in solution can be made. © 2013 Author(s). All article content, except where otherwise noted, is licensed under a Creative Commons Attribution 3.0 Unported License. [<http://dx.doi.org/10.1063/1.4829975>]

Responsive polymers and polymer-based materials,^{1–4} defined as materials that physically and/or chemically “react” to changes in their environment,^{5–7} have garnered significant interest over the last couple of decades for various applications – analytical and biological applications included. Responsive polymers have been made to respond to a number of environmental changes, most commonly temperature, pH, ionic strength, and the concentration of various molecules of interest (e.g., proteins and DNA).^{8–17}

While there are a number of responsive polymers known, poly (*N*-isopropylacrylamide) (pNIPAm) has been the most extensively studied responsive polymer to date.^{18–24} pNIPAm is fully water-soluble and solvated at temperatures below $\sim 32^\circ\text{C}$, and undergoes a volume phase transition to a desolvated (collapsed) state at $T > 32^\circ\text{C}$, which is pNIPAm's lower critical solution temperature (LCST). Furthermore, at $T > 32^\circ\text{C}$ the polymer exists as a globule, while it is in a random coil conformation at $T < 32^\circ\text{C}$. Colloidally stable pNIPAm-based micro and nanoparticles (microgels and nanogels) can also be synthesized, and like their linear counterpart, undergo a solvation state change as a function of temperature. Specifically, pNIPAm-based particles are fully water swollen (large diameter) at $T < 32^\circ\text{C}$, while they are dehydrated (small diameter) at $T > 32^\circ\text{C}$.²²

The synthesis of pNIPAm-based microgels is very straightforward and versatile, allowing for the chemistry of the microgel to be tailored to meet the needs of various applications. They are typically synthesized using free radical precipitation polymerization, where the particles size, porosity, and chemistry can be easily tuned by varying the components in the reaction solution.^{25–27} Microgels with a variety of different functional groups have been synthesized using this approach, simply by adding functional comonomers to the reaction solution.^{26,28,29} The most commonly used comonomer is acrylic acid (AAc),^{30,31} which is particularly interesting because it imparts pH responsivity to the pNIPAm-based microgels. AAc has a pK_a of ~ 4.25 , therefore at $\text{pH} > 4.25$ the AAc groups are deprotonated making the microgels negatively charged, while they are neutral at $\text{pH} < 4.25$ due to AAc protonation. Therefore, at high pH the microgels swell due to the charge-charge (Coulombic) repulsion in the microgel's polymer network. In this case, the pNIPAm-based microgels will be both temperature and pH responsive.³² Another advantage of having AAc present in the microgels is their

^aE-mail: michael.serpe@ualberta.ca

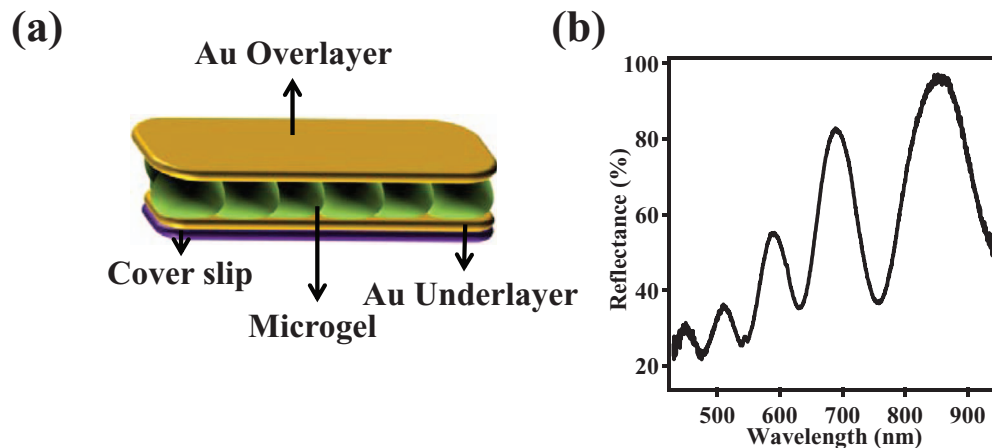


FIG. 1. (a) The basic structure of a microgel-based etalon. The Au overlayer in the figure is drawn as a planar layer, but is actually conformal to the microgel layer. Each Au layer was supported by 2 nm Cr as an adhesion layer. (b) Characteristic reflectance spectra from a pNIPAm-co-AAc microgel-based etalon.

ability to react with other functional small molecules to add further responsivity, and/or functionality to the microgels.^{33–35}

It is well known that when charged pNIPAm-based microgels are in the presence of an oppositely charged polyelectrolyte, it is able to penetrate, crosslink, and cause the microgel to change solvation state. The detailed study of polyelectrolyte and microgel complexation and related chemistry have been reported in a number of papers.^{36–42} Of significant interest to the work here, Richtering and Kleinen³⁶ synthesized poly (*N*-isopropylacrylamide)-*co*-methacrylic acid (pNIPAm-co-MAA) microgels, and showed that they were anionically charged at $\text{pH} > \text{MAA's } \text{pK}_a$.³⁶ Interestingly, they showed that their diameter decreased in the presence of anionic linear polymer (polyanion). The scope of this submission is not to highlight the chemistry of interaction of microgel with oppositely charged polyelectrolyte in solution. This submission focuses on the utilization of this phenomenon to determine the molecular weight (MW) of polyelectrolytes in solution. Our group recently used this phenomenon to probe the ability of macromolecules to enter pNIPAm microgel-based optical devices (i.e., etalons) our lab is developing. Figure 1(a) shows the basic structure of a pNIPAm microgel-based etalon. They are fabricated by “painting” a layer of pNIPAm-based microgels onto a Au-coated glass substrate (typically, 15 nm Au) onto which another Au layer is deposited (typically called a Au overlayer).⁴³ The devices exhibit visual color and distinct multipeak spectra, due to light resonating and interacting in the microgel-based cavity between the Au layers/mirrors.^{44–46} A representative spectrum from a microgel-based etalon can be seen in Figure 1(b). The position of the peaks in the multipeak spectra (λ) can be predicted from Eq. (1),

$$m\lambda = 2nd \cos \theta, \quad (1)$$

where n is the refractive index of the dielectric layer, d is the mirror-mirror distance, θ is the angle of incident light relative to the normal, and m (an integer) is the order of the reflected peak.^{47,48}

Previously, we showed that when charged pNIPAm-based microgels are immobilized between two metal substrates of an etalon, polyelectrolyte of opposite charge is able to penetrate through the etalon’s Au overlayer and crosslink the microgels.^{49,50} This crosslinking resulted in a shift in the etalon’s reflectance peaks. Furthermore, we showed that the ability of the polyelectrolytes to enter the etalon’s cavity depends on the thickness of the Au overlayer and the polyelectrolyte’s MW. Specifically, we found that low MW polyelectrolyte can penetrate through all etalons with the various overlayer thicknesses (5, 15, 25, and 35 nm), whereas high MW polyelectrolyte can only penetrate etalons with thin Au overlayers (e.g., 5 nm). Effectively, the Au overlayer seems to be

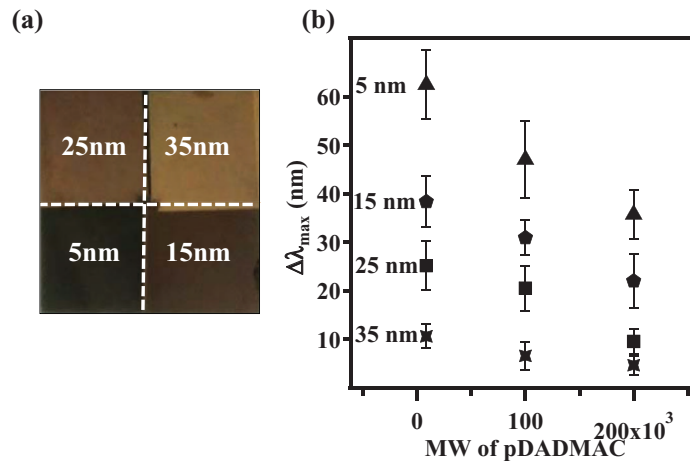


FIG. 2. (a) PNIPAm-co-AAc microgel-based etalon with different Au overlayer thicknesses in different parts of etalon. The device is 1 in. \times 1 in. in dimension. (b) Shift of λ_{\max} for same pNIPAm-co-AAc etalon with different overlayer thickness in pH 6.5 after addition of pDADMAC solution of different MW. The shifts shown in figure are cumulative shift. Each data point represents the average of at least three independent measurements, and the error bars are standard deviation for those values.

acting to “filter” specific MW polyelectrolytes out from solution, and only letting polyelectrolytes with specific MW to enter the microgel layer.

So, we could use this behaviour of polyelectrolyte penetration through Au overlayer to sense the presence of polyelectrolyte in the solution. In this paper, we studied whether etalon arrays (either with different Au overlayers or different microgels) can be used to determine the NW composition and nature of polyelectrolytes by monitoring the individual reflectance spectra. Here, Au overlayer acts as a filter with its average pore size to decide what MW and the extent polyelectrolytes can penetrate to crosslink the microgel in the arrays. Based on the spectral responses we can say the MW of polyelectrolytes in solution. We observed that etalon arrays fabricated with different Au overlayer thicknesses on same etalon can sense the presence of different MW polyelectrolytes independently. Thick Au overlayer regions can sense only small MW polyelectrolytes, whereas thin Au overlayer regions can sense all MW polyelectrolytes. We also found that etalon arrays with different microgels and thicknesses in same etalon can respond to the presence of different polyelectrolytes individually.

Methods are detailed in the supplementary material.⁵¹

Based on our previous studies^{49,50} on the penetration of positively charged polyelectrolyte to the oppositely charged microgel in the etalon, we hypothesize that etalon arrays designed in same etalon can be used to distinguish the presence of composition and MW of polyelectrolytes in solution. This could be done by monitoring the individual spectral response of etalon arrays with different overlayer thicknesses.

Figure 2(a) shows a photograph of a single pNIPAm-co-AAc microgel-based etalon, which has different Au overlayer thicknesses (5, 15, 25, and 35 nm Au) deposited on spatially distinct regions on a single glass substrate. Therefore, we hypothesize that each region will respond to different MW polyelectrolytes. Figure 2(b) shows the spectral response from the individual array elements after a given amount of high MW poly (diallyldimethyl ammonium chloride) (pDADMAC) (MW \sim 200 000) solution was introduced to the chamber containing the anionically charged pNIPAm-co-AAc microgel-based etalon shown in Figure 2(a); the etalon was fully stable in pH 6.5 solution (ionic strength 2 mM with NaCl) before addition. The responses of different etalons, with different Au overlayer thicknesses, were monitored simultaneously and independently. We found that addition of the high MW polyelectrolyte has an unnoticeable or very small influence on the position of the spectral peaks for the etalons with 25 and 35 nm overlayers, while the 5 nm and 15 nm overlayer etalons respond, showing 37 nm and 25 nm shifts in the position of their reflectance peaks, respectively. From this, we can see that the high MW polyelectrolyte can only penetrate the etalon array elements that have a large enough pore size, such that the polyelectrolyte can interact

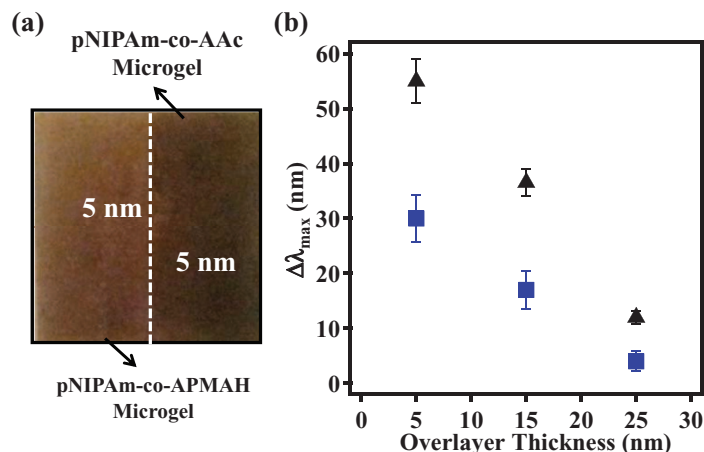


FIG. 3. (a) PNIPAm-co-AAc and pNIPAm-co-APMAH microgel-based etalon with same Au overlayer thickness. (b) Cumulative shift of λ_{\max} for same etalon with same overlayer thickness and different microgel in pH 6.5 after addition of pDADMAC (▲) and PSS (■ (blue)) solution. Each data point represents the average of at least three independent measurements, and the error bars are standard deviation for those values.

with, and collapse, the microgel layer. Furthermore, the extent of collapse depends on how much of the polyelectrolyte can enter the microgel layer, which depends on pore size, controlled by overlayer thickness. Following the stabilization of the etalon array, an addition aliquot of pDADMAC of MW < 100 000 was added to the etalon array, allowed to stabilize and then this was followed by addition of low MW pDADMAC (MW = 8500). The spectral response of each etalon array element was monitored after each pDADMAC addition. As can be seen in Figure 2(b), “medium” and “low” molecular weight polyelectrolytes are able to penetrate the array elements with thick Au overlayers to different extents. We want to make it clear here that the excess polyelectrolyte that did not penetrate the etalons, and that was left in the chamber, was washed away prior to the addition of the next polyelectrolyte. These data show that the etalon arrays are able to respond differentially to various MW polyelectrolytes in solution, and can be used to determine the MW of polyelectrolytes in a solution.

Next, etalon arrays were fabricated with both positively and negatively charged microgels arrayed, spatially isolated, on a single Au coated glass substrate. This was accomplished by painting one half of the Au coated glass substrate with pNIPAm-co-AAc microgels, and another half with pNIPAm-co-*N*-(3-aminopropyl)methacrylamide hydrochloride (pNIPAm-co-APMAH). The same thickness of 5 nm Au was coated as an overlayer on both halves. A photograph of the constructed device is shown in Figure 3(a). We then exposed the etalon, half coated with positively charged microgels, and the other with negatively charged microgels, to low-MW pDADMAC (MW = 8500) and monitored the optical properties of the individual array elements. The data in Figure 3(b) show that the pNIPAm-co-AAc microgel-based etalon array element responded to the pDADMAC addition by shifting 55 nm, while the pNIPAm-co-APMAH microgel-based etalon array element did not exhibit a noticeable shift. After rinsing the chamber to remove the left over pDADMAC, the etalon array was exposed to poly (sodium 4- styrenesulfonate) (PSS) (MW = 70 000). In this case, the array element containing the pNIPAm-co-APMAH microgels shifted 45 nm, while the array element containing pNIPAm-co-AAc exhibited no noticeable shift. It should be noted that the extent of shift is larger for pDADMAC than PSS due to its low MW. Similar to above, when the overlayer thickness was increased, the extent of polyelectrolyte penetration into the array elements was decreased, suggesting again that these could be used for determining the molecular weight of polyelectrolytes in solution, but we can even differentiate based on charge.

Finally, etalons were constructed by painting half of Au coated glass cover slip with pNIPAm-co-AAc and another half with pNIPAm-co-APMAH. Now half of the painted substrate was coated with 5 nm Au and another half with 15 nm Au overlayer such that we get the etalon arrays as shown in photograph of Figure 4(a). A given amount of pDADMAC of MW < 100 000 solution

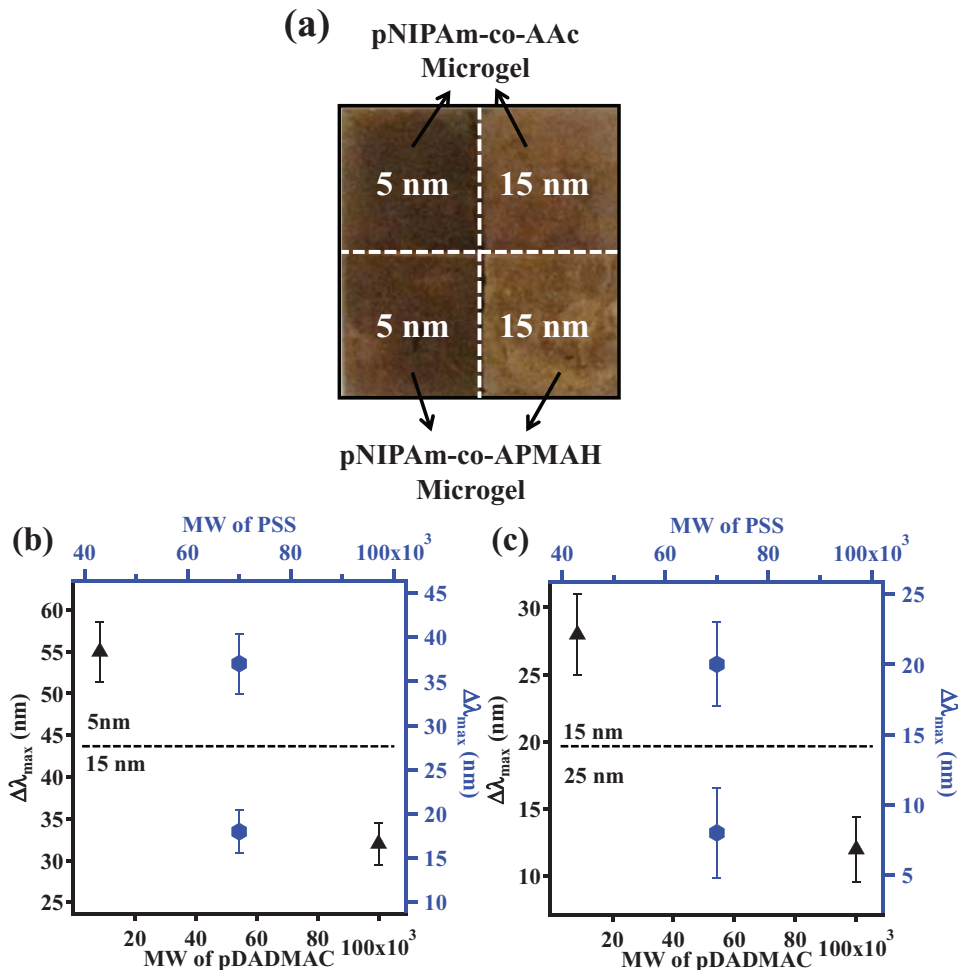


FIG. 4. (a) PNIPAm-co-AAc and pNIPAm-co-APMAH microgel-based etalon with different Au overlayer thicknesses. (b) Cumulative shift of λ_{\max} for same etalon with different overlayer thickness and different microgels in pH 6.5 after addition of pDADMAC solution of different MW and PSS solution. Each data point represents the average of at least three independent measurements, and the error bars are standard deviation for those values.

was exposed to the etalon arrays. We found that a shift of 32 and 17 nm from pNIPAm-co-AAc arrays with 5 nm and 15 nm Au overlayers, whereas pNIPAm-co-APMAH arrays did not show any noticeable change (data not shown). The excess polyelectrolyte was rinsed away and pDADMAC with MW 8500 was exposed to the chamber and the spectral responses were monitored as above. We observed a cumulative shift of 55 nm and 33 nm from pNIPAm-co-AAc arrays with 5 nm and 15 nm overlayer thicknesses (Figure 4(b)), respectively, while the pNIPAm-co-APMAH arrays did not show any significant response. Similarly, same amount of PSS (MW = 70 000) solution exposed to the chamber showed 37 nm and 18 nm shifts with 5 nm and 15 nm overlayers from pNIPAm-co-APMAH arrays shown in Figure 4(b). We also found that etalon arrays fabricated in similar fashion showed selectivity depends on the nature of microgel and Au overlayer thicknesses (Figure 4(c)). So, etalon arrays can be a potential sensor to determine MW and nature of polyelectrolytes in solution.

The device was tested for reusability after regeneration. The regeneration was done by soaking the used pNIPAm-co-AAc etalon with different Au overlayers in pH 3.0 solution for overnight followed by soaking at high ionic strength aqueous solution for 24 h and then soaking in deionized water (DI) water at 35 °C overnight. As can be seen in Figure 5, the performance decreases after regeneration, although the device is still capable of being used over multiple cycles.

In conclusion, we showed that etalon arrays can be fabricated to show selectivity towards different polyelectrolytes. We found that Au overlayers act as a MW filter, which determines what

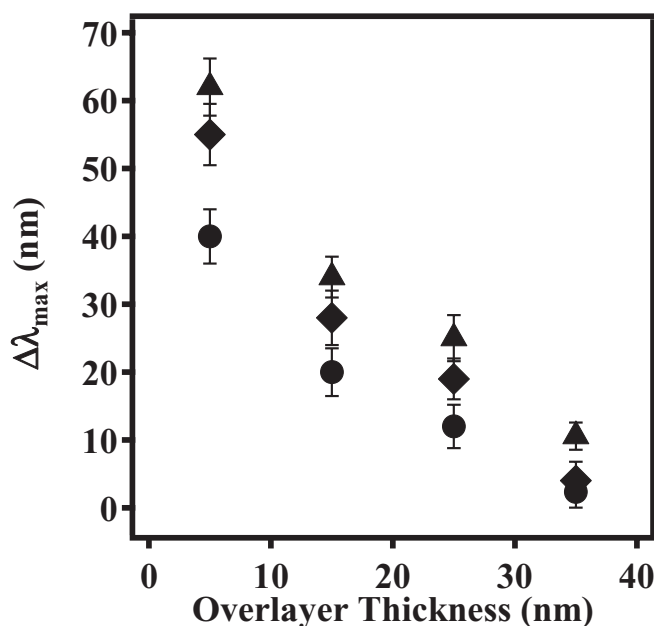


FIG. 5. The shift of λ_{\max} for pNIPAm-co-AAc microgel etalon arrays with different thicknesses for regeneration. Here (▲) represents the peak shift of a new etalon arrays, (◆) represents the peak shift after 1st regeneration, and (●) represents the peak shift after 2nd regeneration.

MW can penetrate the etalon, and interact with the etalon's microgel layer. Due to the penetration of polyelectrolyte and electrostatic interaction with microgel, the reflectance spectrum shifts towards shorter wavelength, the extent of which depends on the number of molecules that penetrate the etalon and MW. This device has the potential to act as a quick, simple, and inexpensive polymer MW sensor.

M.J.S. acknowledges funding from the University of Alberta (the Department of Chemistry and the Faculty of Science), the Natural Science and Engineering Research Council (NSERC), the Canada Foundation for Innovation (CFI), the Alberta Advanced Education & Technology Small Equipment Grants Program (AET/SEGP), and Grand Challenges Canada. M.J.S. acknowledges Mark McDermott for the use of the thermal evaporator.

- ¹J. R. Capadona, K. Shanmuganathan, D. J. Tyler, S. J. Rowan, and C. Weder, *Science* **319**, 1370–1374 (2008).
- ²H. Lee, B. P. Lee, and P. B. Messersmith, *Nature (London)* **448**, 338–342 (2007).
- ³C. M. Haller, W. Buerzle, C. E. Brubaker, P. B. Messersmith, E. Mazza, O.-N. Koelble, R. Zimmermann, and M. Ehrbar, *Prenat Diagn.* **31**, 654–660 (2011).
- ⁴H. Lee, S. M. Dellatore, W. M. Miller, and P. B. Messersmith, *Science* **318**, 426–430 (2007).
- ⁵A. Suzuki and T. Tanaka, *Nature (London)* **346**, 345–347 (1990).
- ⁶A. Gutowska, Y. H. Bae, H. A. Jacobs, J. Feijen, and S. W. Kim, *Macromolecules* **27**, 4167–4175 (1994).
- ⁷R. Pelton, *Adv. Colloid Interface Sci.* **85**, 1–33 (2000).
- ⁸A. L. Black, J. M. Lenhardt, and S. L. Craig, *J. Mater. Chem.* **21**, 1655–1663 (2011).
- ⁹A. Dedinaite, E. Thormann, G. Olanya, P. M. Claesson, B. Nystrom, A. L. Kjoniksen, and K. Z. Zhu, *Soft Matter* **6**, 2489–2498 (2010).
- ¹⁰T. Alizadeh, M. R. Ganjali, and M. Zare, *Anal. Chim. Acta* **689**, 52–59 (2011).
- ¹¹H. Ouyang, Z. H. Xia, and J. A. Zhe, *Microfluid. Nanofluid.* **9**, 915–922 (2010).
- ¹²E. Ayano, M. Karaki, T. Ishihara, H. Kanazawa, and T. Okano, *Colloids Surf., B* **99**, 67–73 (2012).
- ¹³M. A. Nash, J. N. Waitumbi, A. S. Hoffman, P. Yager, and P. S. Stayton, *ACS Nano* **6**, 6776–6785 (2012).
- ¹⁴N. Morimoto, X. P. Qiu, F. M. Winnik, and K. Akiyoshi, *Macromolecules* **41**, 5985–5987 (2008).
- ¹⁵V. V. Yashin, O. Kuksenok, and A. C. Balazs, *Prog. Polym. Sci.* **35**, 155–173 (2010).
- ¹⁶E. S. M. Lee, B. Shuter, J. Chan, M. S. K. Chong, J. Ding, S. H. Teoh, O. Beuf, A. Briguët, K. C. Tam, M. Choolani, and S. C. Wang, *Biomaterials* **31**, 3296–3306 (2010).
- ¹⁷W. Fischer, M. A. Quadir, A. Barnard, D. K. Smith, and R. Hagg, *Macromol. Biosci.* **11**, 1736–1746 (2011).
- ¹⁸J. D. Debord and L. A. Lyon, *Langmuir* **19**, 7662–7664 (2003).
- ¹⁹T. Hoare and R. Pelton, *Macromolecules* **40**, 670–678 (2007).
- ²⁰J. Kleinen and W. Richtering, *J. Phys. Chem. B* **115**, 3804–3810 (2011).

- ²¹ H. Kawaguchi, K. Fujimoto, and Y. Mizuhara, *Colloid Polym. Sci.* **270**, 53–57 (1992).
- ²² C. Wu and S. Zhou, *Macromolecules* **28**, 8381–8387 (1995).
- ²³ M. J. Serpe and L. A. Lyon, *Chem. Mater.* **16**, 4373–4380 (2004).
- ²⁴ G. Zhang and C. Wu, *J. Am. Chem. Soc.* **123**, 1376–1380 (2001).
- ²⁵ M. J. Serpe, C. D. Jones, and L. A. Lyon, *Langmuir* **19**, 8759–8764 (2003).
- ²⁶ D. J. Gan and L. A. Lyon, *Macromolecules* **35**, 9634–9639 (2002).
- ²⁷ Z. Y. Meng, J. K. Cho, S. Debord, V. Breedveld, and L. A. Lyon, *J. Phys. Chem. B* **111**, 6992–6997 (2007).
- ²⁸ K. Kratz, T. Hellweg, and W. Eimer, *Colloids Surf., A* **170**, 137–149 (2000).
- ²⁹ S. Zhou and B. Chu, *J. Phys. Chem. B* **102**, 1364–1371 (1998).
- ³⁰ A. Burmistrova and R. von Klitzing, *J. Mater. Chem.* **20**, 3502–3507 (2010).
- ³¹ C. D. Jones and L. A. Lyon, *Macromolecules* **33**, 8301–8306 (2000).
- ³² G. E. Morris, B. Vincent, and M. J. Snowden, *J. Colloid Interface Sci.* **190**, 198–205 (1997).
- ³³ M. Karg and T. Hellweg, *Curr. Opin. Colloid Interface Sci.* **14**, 438–450 (2009).
- ³⁴ S. Nayak, H. Lee, J. Chmielewski, and L. A. Lyon, *J. Am. Chem. Soc.* **126**, 10258–10259 (2004).
- ³⁵ S. Schmidt, T. Hellweg, and R. von Klitzing, *Langmuir* **24**, 12595–12602 (2008).
- ³⁶ J. Kleinen and W. Richtering, *Colloid Polym. Sci.* **289**, 739–749 (2011).
- ³⁷ E. A. Karpushkin, S. B. Zezin, and A. B. Zezin, *Polym. Sci., Ser. A Ser. B* **51**, 33–37 (2009).
- ³⁸ A. B. Zezin, V. B. Rogacheva, and V. A. Kabanov, *Macromol. Symp.* **126**, 123–141 (1998).
- ³⁹ V. A. Kabanov, A. B. Zezin, V. B. Rogacheva, T. V. Panova, E. V. Bykova, J. G. H. Joosten, and J. Brackman, *Faraday Discuss.* **128**, 341–354 (2005).
- ⁴⁰ A. R. Khokhlov, E. Y. Kramarenko, E. E. Makhaeva, and S. G. Starodubtzev, *Macromolecules* **25**, 4779–4703 (1992).
- ⁴¹ V. A. Kabanov, V. B. Skobeleva, V. B. Rogacheva, and A. B. Zezin, *J. Phys. Chem. B* **108**, 1485–1490 (2004).
- ⁴² D. A. Davydov, E. G. Yaroslavova, A. A. Efimova, and A. A. Yaroslavov, *Colloid J.* **71**, 55–62 (2009).
- ⁴³ C. D. Sorrell, M. C. D. Carter, and M. J. Serpe, *ACS Appl. Mater. Interfaces* **3**, 1140–1147 (2011).
- ⁴⁴ C. D. Sorrell, M. C. D. Carter, and M. J. Serpe, *Adv. Funct. Mater.* **21**, 425–433 (2011).
- ⁴⁵ C. D. Sorrell and M. J. Serpe, *Adv. Mater.* **23**, 4088–4092 (2011).
- ⁴⁶ M. C. D. Carter, C. D. Sorrell, and M. J. Serpe, *J. Phys. Chem. B* **115**, 14359–14368 (2011).
- ⁴⁷ G. Brooker, *Modern Classical Optics* (Oxford University Press, Oxford, U.K., 2003).
- ⁴⁸ J. M. Vaughan, *The Fabry-Perot Interferometer: History, Theory, Practice and Applications* (Taylor and Francis Group, New York, 1989), p 583.
- ⁴⁹ M. R. Islam and M. J. Serpe, *Macromolecules* **46**, 1599–1607 (2013).
- ⁵⁰ M. R. Islam and M. J. Serpe, *Chem Commun.* **49**, 2646–2648 (2013).
- ⁵¹ See supplementary material at <http://dx.doi.org/10.1063/1.4829975> for experimental details including microgel synthesis, etalon array fabrication, and MW selectivity and sensing experiment.